INTEGRATING DIFFRACTIVE REAR SIDE STRUCTURES FOR LIGHT TRAPPING INTO CRYSTALLINE SILICON SOLAR CELLS

J. Eisenlohr[1*], H. Hauser[1], J. Benick[1], A. Mellor[2], B. Bläsi[1], J.C. Goldschmidt[1], M. Hermle[1]
[1]Fraunhofer Institute for Solar Energy Systems, Heidenhofstr. 2, 79110 Freiburg, Germany
[2]Instituto de Energia Solar, Universidad Politecnica de Madrid, Avenida Complutense 30, Madrid 28040, Spain
[*]johannes.eisenlohr@ise.fhg.de

ABSTRACT:
Diffractive rear side light trapping structures significantly enhance the path length for near infrared light. We present a way of integrating such diffractive rear side structures into crystalline silicon solar cells. Two types of diffractive structures, hexagonal sphere gratings and binary gratings have been simulated and fabricated. For both structures absorption enhancements corresponding to a photo current density gain of 1-2 mA/cm^2 have been verified in optical measurements. To integrate these diffractive structures into fully processed silicon solar cells, we developed a passivation concept using a thin Al_2O_3 layer that provides a high-quality passivation for the rear side of the active silicon bulk and has a negligible influence on the optical properties. We also present a planarization process that prevents parasitic absorption in the rear side metal layer.
Keywords: Absorption, Light Trapping, Optical Losses

1 INTRODUCTION

Silicon solar cells suffer from losses due to weak absorption of photons in the near infrared (NIR), as the penetration depth of those photons exceeds typical cell thicknesses. To enhance absorption, the effective path length within the solar cell has to be increased for the photons in the NIR. With solar cells becoming thinner, absorption losses increase and light trapping becomes even more essential. Several analytical and numerical investigations indicated that diffractive structures could achieve efficient light trapping [1-4].

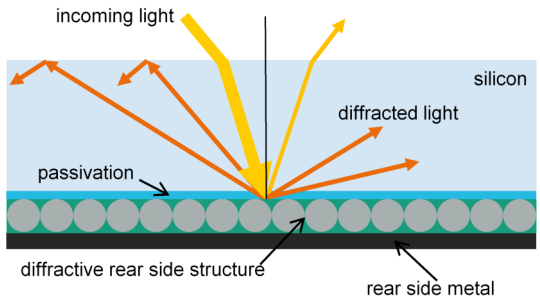

Figure 1: Solar cell concept with a diffractive rear side structure. A thin passivation layer separates the active silicon bulk and the diffractive structure. Here the sphere grating is shown. The light path length in the silicon is enhanced when light is diffracted into non-zero orders. In case of a planar front side light with angles bigger than 16° is totally internally reflected at the front side. The concept for binary gratings is analogous.

Current silicon solar cells usually have a front side texture. For very thin solar cells (40 µm, for instance) however, a front side texture alone may be insufficient and technologically challenging. To achieve sufficient absorption in such thin solar cells, new concepts are required. Diffractive structures on the rear side are one promising approach to enhance internal light path lengths. It is essential to maintain good electrical properties of the solar cell while optimizing the optical properties. Therefore we propose a very thin passivation layer between the active silicon bulk and the diffractive rear side. A schematic sketch of the solar cell structure is showed in Figure 1. We investigated diffractive rear side structures with optical simulations and we present two concepts for the realization of such structures for silicon solar cells: first, self-ordered hexagonal sphere gratings and second, gratings produced via nano-imprint lithography (NIL). We verified absorption enhancements for both structures and investigated surface passivation and electrical contact formation.

2 EVALUTATION OF DIFFERENT LIGHT TRAPPING CONCEPTS

To evaluate different light trapping structures we conducted optical simulations using the transfer matrix method [5], rigorous coupled wave analysis [6, 7] and Sentaurus Device [8]. We calculated the absorption in solar cells with planar front and rear side, in solar cells with inverted pyramids on the front side and a planar rear side and in solar cells with a planar front and a hexagonal sphere grating on the rear side. As a benchmark we also included lambertian scatterers, for which we calculated the absorption according to [9]. It has to be mentioned that the intensity and hence the absorption enhancement due to a lambertian scatterer is not exactly the famous $4n^2$-limit but considerably smaller because of the non-zero absorption of silicon in the relevant spectral range (NIR). As an aggregated number that is easily conceivable and allows comparison to other works, we calculated the maximal achievable photocurrent density j_{ph}, which is possible under illumination with the AM1.5g norm solar spectrum and the simulated absorption A when an internal quantum efficiency of unity is assumed via:

$$j_{ph} = e_0 \int_{\lambda=0}^{\lambda=1200nm} d\lambda \; N_{AM1.5}(\lambda) \; A(\lambda)$$

where $N_{AM1.5}$ denotes the number of photons per area and wavelength and e_0 the charge of an electron. The results displayed in Figure 2 show that especially for thin solar cells the achievable current densities decrease due to weak absorption and hence there is a need for light trapping measures. The optimized hexagonal sphere grating leads to current densities comparable to a solar cell with inverted pyramids. This underlines the potential of diffractive rear side structures, especially for thin solar cells where pyramidal textures are more difficult to

realize.

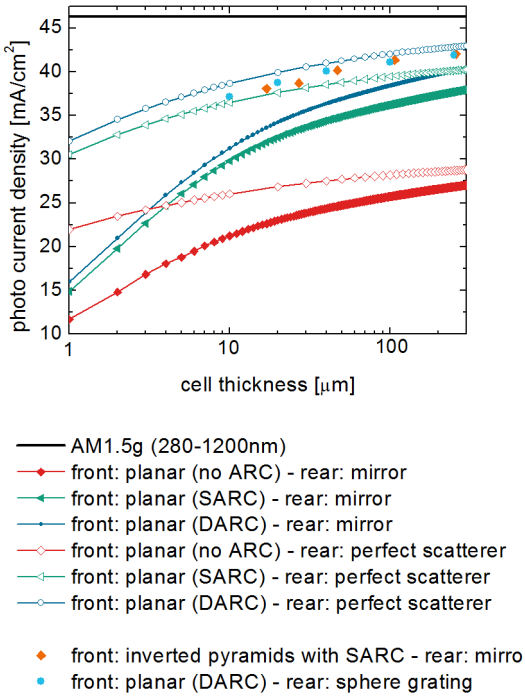

Figure 2: Photo current densities for different light trapping concepts and different cell thicknesses. The three lines with filled symbols represent cells with a planar front side and a perfect mirror on the rear and different planar antireflection coatings (no layer – no ARC, single layer – SARC and double layer – DARC). For thick solar cells the reflection losses at the front side are the main loss mechanism, but for thinner cells the absorption losses gain in importance. These absorption losses are significantly reduced by a lambertian scatterer at the rear side, which is shown by the three lines with open symbols. The orange diamond shaped symbols show cells with inverted pyramids at the front side and a rear mirror. The blue circles represent cells with a planar double layer antireflection coating at the front and an optimized hexagonal sphere grating at the rear.

3 HEXAGONAL SPHERE GRATINGS

One way to realize a diffractive rear side structure is the use of monodisperse silica spheres (for further details see [10]). The fabrication of the sphere grating consists of two steps. First we spin coated the spheres [11] (dispersed in a solution of water and 2-propanol, sphere diameter 922 nm) onto the passivated rear side of silicon wafers with a rotation speed of 4000 rpm. By self-determined growth a hexagonally ordered monolayer builds up. There are still some dislocations or voids in the hexagonal pattern. These lattice defects are a deviation from the simulated hexagonal grating, but they are not necessarily a change for the worse because they cause scattering instead of diffraction. Scattering also causes a light path length enhancement compared to a specular rear side. In the second step the monolayer of spheres can be inverted by infiltrating the voids between the spheres with a high refractive index material (Figure 3). For lab-scale examinations we chose atomic layer deposition of TiO_2, but also potentially cheap sol-gel processes are a promising approach. The deposited TiO_2-layer has a refractive index of 2.4 at 1000 nm, which is significantly higher than the refractive index of the SiO_2-spheres (1.5).

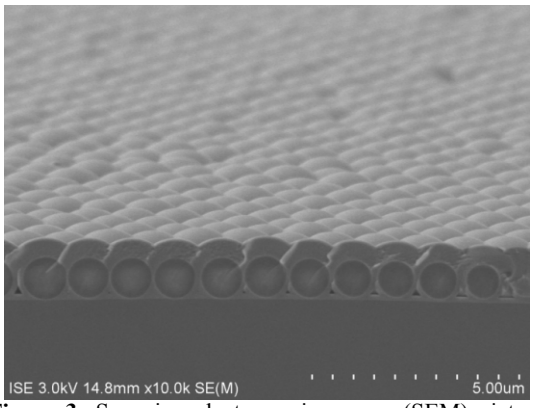

Figure 3: Scanning electron microscope (SEM) picture of a hexagonally ordered monolayer of SiO_2-spheres with a diameter of 922 nm. The spin coating process works homogenously on a 4 inch wafer. The voids have been infiltrated with TiO_2 by atomic layer deposition.

3.1 Passivation Concept

We realized the passivation of the rear side of the solar cell by depositing a very thin Al_2O_3-layer (10 nm). This layer is optically negligible but passivates the rear side effectively. For p-type Si-Wafers (float zone, 1 Ωcm, thickness 250 µm) passivated by 10 nm of Al_2O_3 on both sides life times of over 1 ms were measured. We repeated the measurements after the deposition of TiO_2 and found no deterioration of the passivating properties. The spin coating of the spheres itself and the planarisation of the rear side before the metallization are also considered to be not critical for the passivation layer. Thus the passivating properties of the rear side and the optical properties are separated.

3.2 Planarization

In a final solar cell, a metallic layer is needed for contact formation and as rear reflector. If this metal layer is structured according to the structure of the sphere grating, strong parasitic absorption will occur due to plasmonic effects [12]. Therefore, an additional dielectric buffer layer (DBL) is needed that planarizes the grating structure and creates a flat rear surface on which the metal can be deposited. Therefore we developed a spin coating process of SiO_2-nanoparticles (average size 7 nm) dispersed in water that planarizes the surface after the inversion process. Figure 4 shows a SEM cross-section of the sphere grating after the planarization process.

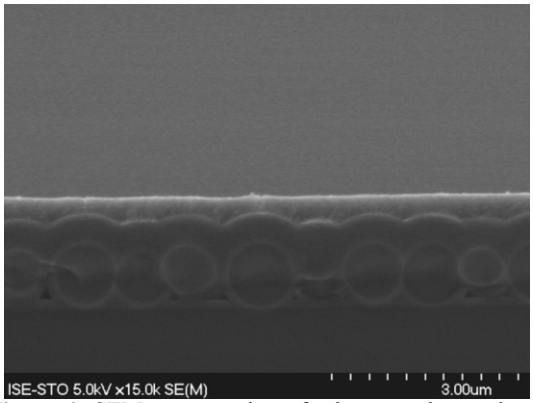

Figure 4: SEM cross section of a hexagonal monolayer of SiO_2-spheres with a diameter of 922 nm. Due to the conformal TiO_2-deposition a structured surface remains after the inversion process. Therefore we spin coated an additional SiO_2-layer, which provides a flat surface.

3.3 Confirmation of absorption enhancement

Using Rigorous Coupled Wave Analysis (RCWA) it has been shown that for planar silicon solar cells significant current density gains can be reached by applying a monolayer of hexagonally ordered SiO_2-spheres embedded in a high refractive index material to the rear side of the cell. We investigated the influence of the sphere diameter and found maximum absorption enhancements for a diameter of about 1 µm [10]. For this diameter the first order of diffraction (for near infrared light) is still totally internally reflected at the flat front surface of the cell. For optimized sphere gratings (matrix material silicon, sphere diameter 1100 nm) we found photo current density gains of over 3 mA/cm^2 for silicon solar cells with a thickness of 40 µm and over 2 mA/cm^2 for 100 µm thick cells. The fabricated system shown in Figure 3 (hexagonally ordered SiO_2-spheres in TiO_2-matrix at the rear of a planar silicon wafer) has been characterized by absorption measurements in an integrating sphere using a Cary5000i from Varian. The measured absorption enhancement in the near infrared is shown in Figure 5. It corresponds to a photo current density gain of 1.49 mA/cm^2 (cell thickness 100 µm, photo current density without sphere grating 35.9 mA/cm^2) and 1.04 mA/cm^2 (cell thickness 250 µm, photo current density without sphere grating 37.3 mA/cm^2). Due to the absorption enhancement the absorption in a wafer with a thickness of 100 µm with the sphere grating exceeds the absorption in a planar wafer with a thickness of 250 µm. This highlights the potential of the proposed light trapping concept with regard to thinner solar cells.

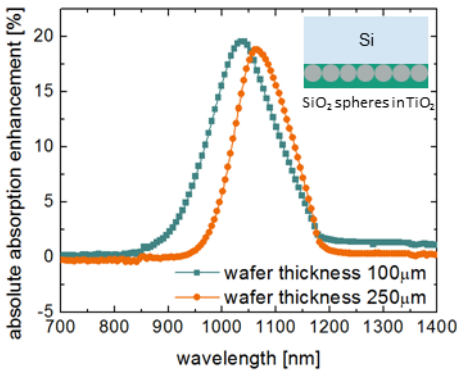

Figure 5: Measured absorption enhancement due to a hexagonal sphere grating at the rear side of a planar silicon wafer compared to a flat rear side. For thinner wafers the absorption enhancement appears already for smaller wavelengths. For wavelengths bigger than 1200 nm there is no absorption enhancement because the absorption coefficient of crystalline silicon approaches zero and even a considerable light path length enhancement does not lead to absorption.

4 BINARY GRATINGS VIA NANO-IMPRINT-LITHOGRAPHY

The second way to realize a diffractive rear side structure is a nano-imprinting process. Similar to the sphere grating the solar cell concept again provides a separation of the electrical and optical properties of the rear side. Hence, the rear side is passivated by a 10 nm thin Al_2O_3-layer as well. On top of this layer we sputtered an amorphous silicon layer into which the grating is etched. This approach has several advantages. First, electrical and optical properties are separated, second, absorption in the grating structure is negligible because amorphous silicon has a larger band-gap than crystalline silicon and third the real part of the refractive index of amorphous silicon is very close to crystalline silicon which leads to high efficiencies concerning the incoupling of the diffracted light. We chose sputtering as deposition method because it is possible to deposit hydrogen free, stable amorphous silicon layers on Al_2O_3. The grating formation is done by nano-imprint lithography [13] in the following steps: first a photoresist is spin coated onto the amorphous silicon. Second a transparent PDMS-stamp, replicated from a master structure that was produced by interference lithography [14], is pressed onto the photoresist and exposed to UV light (NIL). This leaves a replica of the master structure on the photoresist. Third the structure is transferred to the amorphous silicon by an anisotropic reactive ion etching process (RIE). In the last step the remaining resist has to be removed, which is done in an oxygen plasma or in a wet chemical step. A crossed grating fabricated by this process chain is shown in Figure 6:

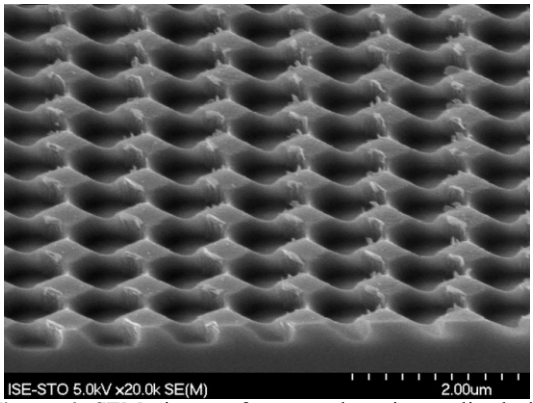

Figure 6: SEM picture of a crossed grating realized via nano-imprint lithography. The grating period is 1 µm and the grating depth approximately 200 nm [15].

4.1 Passivation Concept

Analogous to the sphere gratings the passivation of the rear side was realized with a 10 nm thin Al_2O_3-layer. We conducted life time measurements by quasi steady state photo conductance to investigate the influence of the different process steps. Figure 7 shows the measured life times after each process step. Neither a single process step nor the whole process chain leads to reduced life times. Hence the separation of electrical passivation and optical properties of the rear side was successful.

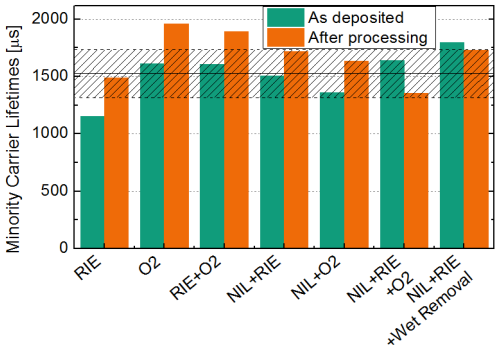

Figure 7: Minority carrier lifetime measurements were conducted before and after each fabrication step of the NIL-gratings. "As deposited" refers to samples after the deposition of the passivation layer and the amorphous silicon layer, but before the fabrication steps of the grating. The black line indicates the mean value of these measurements and the dashed area the statistic error. All fabrication steps of the grating (reactive ion etching RIE, oxygen plasma ashing O_2, wet-chemical removal of photoresist) were examined individually on different wafers. All steps and the full process chain have no measurable influence on the lifetime.

4.2 Planarization

Also for the binary gratings an additional dielectric buffer layer is needed to avoid parasitic absorption in the metal rear contact. Therefore we used a similar spin coating process than in the case of sphere gratings. Figure 8 shows a cross section of a planarized grating structure. On top of the planar SiO_2-layer the metal rear reflector can be deposited.

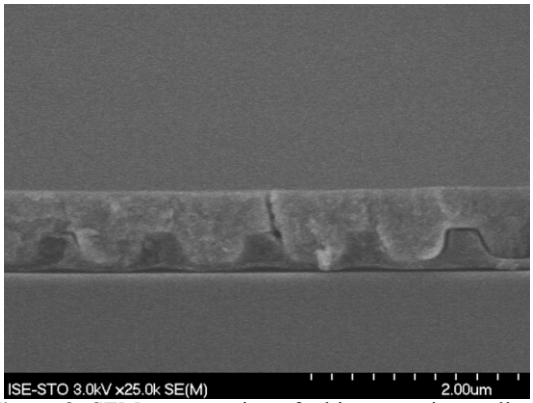

Figure 8: SEM cross section of a binary grating realized via nano imprint lithography. The structured surface has been planarized with SiO_2 in a spin coating process to avoid parasitic absorption in the rear side metal layer that has to be deposited on top of the diffractive structure in a final solar cell. Shown here is not the final grating in silicon but a test sample with structured photoresist [13].

4.3 Contact Formation

In order to realize electrical contacts on the rear side openings have to be created in the diffractive structures. Laser processes are one promising possibility. Additionally we identified a lab-scale process using photolithography and different etching steps. By combining plasma etching and wet chemical etching, the three layers Al_2O_3, a-Si and SiO_2 can be etched selectively and defined contact holes can be realized.

4.4 Confirmation of absorption enhancement

Analogous to the sphere gratings the absorption enhancement due to the diffractive rear side structure has been verified by spectrophotometric measurements. The measured absorption enhancement corresponds to a photo current density gain of 1.6 mA/cm^2 and is thus in the same range than for the sphere gratings. For the details at this point we refer to [15]. This detailed analysis also quantifies the parasitic losses due to a structured metal rear reflector. In Figure 9 simulation results and measurements for crossed and line gratings are shown. The top left graph shows the flat reference wafer with planar front and rear side. The absorption is separated into "useful" absorption in the silicon bulk and parasitic absorption in the rear side metal by a simulation method presented in [16]. Insert A shows the results for a crossed grating, where no planarization was done. A significant part of the total absorption enhancement is parasitic absorption in the Aluminum. Inserts B, C and D show results for line gratings with increasing planarization. The parasitic absorption is reduced while the absorption in the Silicon increases. This underlines the need for a planarized dielectric buffer layer.

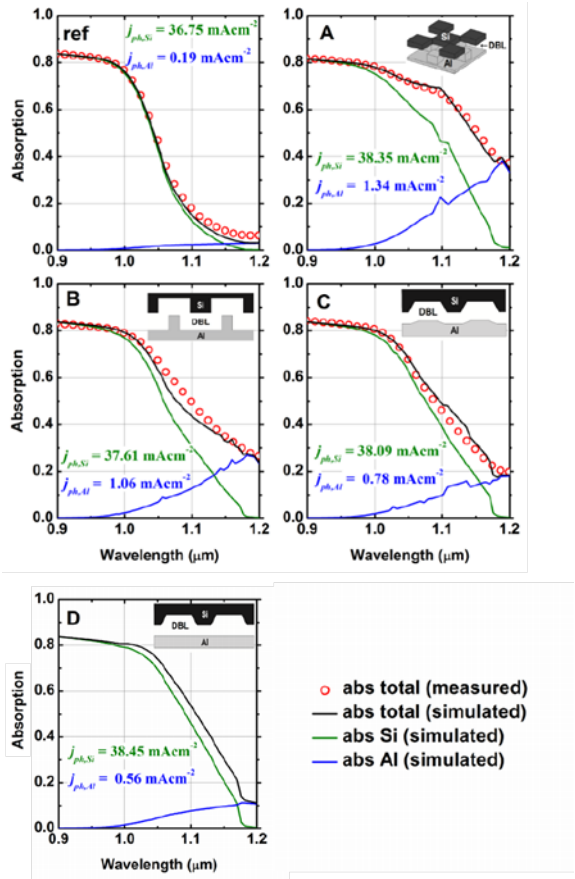

Figure 9: Calculated and measured absorption spectra of 200 µm thick wafers with binary gratings on the rear side. The measured absorption is shown by the red circles, the simulated total absorption by the black line and the simulated absorption in the silicon and aluminum by green and blue lines [15].

5 SUMMARY AND OUTLOOK

By calculations for varying cell thicknesses we showed that especially thin solar cells require light trapping concepts. Diffractive rear side structures are able to enhance light path lengths in the near infrared significantly and we showed that for planar front sides and diffractive rear sides photo current densities comparable to cells with inverted pyramids on the front and a planar rear side are possible. Especially because pyramidal texturing gets more and more difficult for thinner wafers, diffractive rear sides are a promising alternative. We fabricated sphere gratings consisting of monodisperse SiO_2-spheres and a high-refractive index matrix, which was realized by atomic layer deposition of TiO_2. Furthermore we fabricated binary gratings using nano-imprint lithography. For both grating types absorption measurements confirm an absorption enhancement in the near infrared. To separate the optical properties of the rear side from the electrical, we integrated a thin Al_2O_3 passivation layer between the silicon bulk and the diffractive structures. By minority carrier life time measurements we showed that the fabrication steps of both grating types do not affect the passivation. Because a rear side metal layer is needed in a final solar cell we applied a dielectric buffer layer that planarizes the rear side. Therefore spin coating of SiO_2-nanoparticles has been used. A further challenge that has to be solved for integration of diffractive rear side structures into complete solar cells is the contact formation. Laser processes as well as photolithography are promising possibilities and require further investigations.

6 ACKNOWLEDGEMENT

The research leading to these results has received funding from the German Federal Ministry of Education and Research in the project “InfraVolt” (project number 03SF0401B) and from the German Federal Ministry for the Environment, Nature Conservation and Nuclear Safety under contract number 0325292 “ForTeS”. The authors also thank Beneq for atomic layer depositions. Johannes Eisenlohr gratefully acknowledges the scholarship support from the Deutsche Bundesstiftung Umwelt DBU.

REFERENCES

[1] Sheng, P., A.N. Bloch, and R.S. Stepleman, *Wavelength-selective absorption enhancement in thin-film solar cells.* Applied Physics Letters, 1983. **43**(6): p. 579-581.

[2] Peters, I.M., *Photonic concepts for solar cells*, in *Faculty of Mathematics and Physics*. 2009, Universität Freiburg: Freiburg, Germany. p. 202.

[3] Heine, C. and R.H. Morf, *Submicrometer gratings for solar energy applications* Applied Optics, 1995. **34**(14): p. 2476-82.

[4] Bermel, P., C. Luo, L. Zeng, L.C. Kimerling, and J.D. Joannopoulos, *Improving thin-film crystalline silicon solar cell efficiencies with photonic crystals.* Optics Express, 2007. **15**(25): p. 16986-17000.

[5] Mcleod, H.A., *Thin Film Optical Filters.* 2001. **3rd Edition**.

[6] Moharam, M.G. and T.K. Gaylord, *Rigorous coupled-wave analysis of planargrating diffraction.* J. Opt. Soc. Am., 1981. **71**: p. 811–818.

[7] Lalanne, P. and M.P. Jurek, *Computation of the near-field pattern with the coupled wave method for transverse magnetic polarization.* J. Mod. Optics, 1998. **45**: p. 1357-1374.

[8] Sentaurus TCAD, *Technology computer aided design (TCAD)*, Synopsys: Zürich, Switzerland.

[9] Yablonovitch, E., *Statistical ray optics.* Journal of the Optical Society of America, 1982. **72**(7): p. 899-907.

[10] Eisenlohr, J., J. Benick, M. Peters, B. Bläsi, J.C. Goldschmidt, and M. Hermle, *Hexagonal Sphere Gratings for Enhanced Light Trapping in Silicon Solar Cells.* submitted to Optics Express, September 2013.

[11] Nanoparticles produced by MicroParticles GmbH, www.microparticles.com.

[12] Kim, S.-K., H.-S. Ee, W. Choi, S.-H. Kwon, J.-H. Kang, Y.-H. Kim, H. Kwon, and H.-G. Park, *Surface-plasmon-induced light absorption on a rough silver surface.* Applied Physics Letters, 2011. **98**(1): p. 011109.

[13] Hauser, H., A. Mellor, A. Guttowski, C. Wellens, J. Benick, C. Müller, M. Hermle, and B. Bläsi, *Diffractive backside structures via nanoimprint*

lithography. Energy Procedia, 2012. **27**(0): p. 337-342.

[14] Wolf, A.J., H. Hauser, V. Kübler, C. Walk, O. Höhn, and B. Bläsi, *Origination of nano- and microstructures on large areas by interference lithography*. Microelectronic Engineering, 2012. **98**(0): p. 293-296.

[15] Mellor, A., H. Hauser, C. Wellens, J. Benick, J. Eisenlohr, M. Peters, A. Guttowski, I. Tobías, A. Martí, A. Luque, and B. Bläsi, *Nanoimprinted diffraction gratings for crystalline silicon solar cells: implementation, characterization and simulation*. Optics Express, 2013. **21**(S2): p. A295.

[16] Mellor, A., I. Tobias, A. Marti, and A. Luque, *A numerical study of Bi-periodic binary diffraction gratings for solar cell applications*. Solar Energy Materials and Solar Cells, 2011. **95**(12): p. 3527-3535.